Surface Soil Moisture Estimate by Integration of Optical Remote Sensing and Low-Cost Field Sensor Network: The Case Study of Ceriana-Mainardo (Liguria, Italy)

Alessandro Iacopino(✉), Rossella Bovolenta, and Bianca Federici

Department of Civil, Chemical and Environmental Engineering (DICCA), University of Genoa, Genoa, Italy
{alessandro.iacopino,rossella.bovolenta,
bianca.federici}@unige.it

Abstract. Surface Soil Moisture (SSM) is a fundamental information in various research contexts. The monitoring of soil moisture variations can be performed through an accurate use of sensors calibrated and distributed over the study areas. Also, remote sensing techniques can be used to estimate SSM, analyzing wide areas automatically. Starting from previous studies about the response of capacitive soil moisture sensors (WaterScout SM100) installed in the study area of Ceriana-Mainardo (Liguria, Italy), the present work aims to investigate the correlation between ground-based soil moisture data and reflectance extracted from Sentinel-2 images in a study area characterized by sparsely vegetated surfaces. Despite S-2 limitations due to sensitivity to atmospheric obstacles, they provide very effective monitoring of vegetation conditions, thanks to the Red Edge bands. In fact, Reflectance – Soil Moisture correlation analysis highlighted a better response for Red Edge 2, Red Edge 3, Broad Near Infrared and Near Infrared bands, being the vegetation cover spectral response an indirect indicator of soil moisture in the investigated depths. The best correlation is found referring to soil moisture at 10 cm depth and considering the mean reflectance of the four mentioned bands. This kind of dependency allows to have a quite good correlation ($R^2 = 0.56$, RES STD = 3.3% θ (m^3/m^3), MAE = 2.1% θ (m^3/m^3)), comparable with the accuracy of the ground soil moisture sensors (3% θ), hence useful to extract spatially distributed information of Volumetric Water Content (θ [m^3/m^3%]) from S-2 images. The results of the analysis appear encouraging. The workflow, implemented on an area mostly characterized by complex cultivations, could be replicated on other vegetated land uses in presence of field soil moisture data in the study area.

Keywords: Volumetric Water Content · Monitoring Network · Multispectral Images

E. Borgogno-Mondino and P. Zamperlin (Eds.): ASITA 2024, CCIS 2463, pp. 3–19, 2025.
https://doi.org/10.1007/978-3-031-91141-5_1

1 Introduction

Knowledge of Soil Moisture (SM) (typically referred to the upper meter depth) is useful in several research fields, particularly in hydrological balances [1–3] and precision agriculture [4], but also in the analysis of the mechanical behavior of partially saturated soils on slopes susceptible to surface landslides [5, 6]. It can be distinguished in Surface Soil Moisture (SSM, referring to the first 5–10 cm depth from ground level) and Root Zone Soil Moisture (RZSM, referring to depths between 50–100–200 cm) [7, 8]. SSM estimate (typically expressed in Volumetric Water Content, θ [m^3/m^3%]) can be carried out using sensors (direct measurements) installed in the ground or remote sensing techniques.

Soil moisture sensors, often integrated in monitoring networks consisting of many measuring points (nodes), provide information on the volumetric soil water content locally. Such systems differ based on sensor complexity, accuracy and cost. Some typical examples of soil moisture sensors are gamma-ray transmission, electrical resistance, soil heat flux, time-domain reflectometry (TDR), and frequency-domain reflectometry (FDR) [9, 10]. However, capacitive sensors are more suited for automated applications because of their more straightforward data output, the reduced power consumption, and the lower costs [11].

In order to obtain a spatially distributed estimate of SSM, remote sensing products derived by multispectral optical or microwave radar images, that differ mainly in spatial resolution and sensitivity to atmospheric obstacles [12], can be used. Copernicus Sentinel mission, developed by the European Commission and the European Space Agency for the Copernicus Global Earth Observation Project, have been providing Earth Observation (EO) products for almost a decade. The Sentinel-1 (S-1) imaging system operates in the C-band and has four imaging modes, providing technical support for long-term monitoring of a given region due to its dual polarization capability, short revisit period, and fast processing of products [13]. Sentinel-2 (S-2) satellite carries a high-resolution MultiSpectral Imager (MSI) with 13 spectral bands, three of which are specialized Red Edge bands, particularly effective for monitoring vegetation healthy state [14]. Several studies have relied on the combined use of S-1 and S-2 products to assess surface soil characteristics such as water content, but also organic carbon and total nitrogen [15–17]. However, in this work, because of the marked presence of low vegetation, i.e. herbaceous and shrub species in the study area, classified in the Land Cover cartography [18] as *complex agriculture*, only the potential of S-2 is investigated. Moreover, since the vegetation can be considered homogeneous in the study area, its spectral response can also be considered homogeneous, simplifying the analysis, as described in the following.

The analyzed study area is Ceriana-Mainardo (IM), in the western side of the Ligurian Region, in Italy. The site has been monitored placing in field a network of capacitive sensors (WaterScout SM100), because the area was subject to shallow landslides induced by changes in soil moisture. This occurred, for example, during intense rainfall in 2018, causing road disruption and substantially isolating the population, that was then evacuated from their houses for safety reasons. In such cases, the analysis of the evolution of soil moisture (in the upper meter depth) over time could be useful to assess when conditions become stable again, allowing people to return to their houses.

This paper aims at defining an expeditious methodology for large-scale and high spatial resolution estimate of Surface Soil Moisture, based on the integration of direct ground-based measurements and S-2 multispectral images. The combined use of these resources could lead to a detailed estimate of spatial-temporal variation of SSM, useful for the implementation of geotechnical models for shallow landslide analysis.

The specific goals of the present work can be summarized as follows:

- Correct functionality assessment of the ground-based soil moisture monitoring network; this crucial phase aims to establish the ground-truth, necessary to correlate the satellite images reflectance with the soil moisture measurements.
- Definition of the Reflectance – SM correlation at different multispectral bands, and determination of the spectral bands providing the statistically best correlation (evaluated based on the highest coefficient of determination R^2 values from linear regressions).
- Creation of SM maps from multispectral images, here proposed with reference to homogeneous land uses.

2 Study Area and Ground-Based Data

The Ceriana Mainardo site is one of five landslide areas selected in the Ad-Vitam project (Analysis of the Vulnerability of the Mediterranean Alpine Territories to natural risks), financed within the Interreg V-A France–Italie, ALCOTRA 2014–2020. The aim was to increase the resilience of territories affected by rain-induced shallow landslides through the implementation of a forecasting system based on low-cost environmental monitoring that would provide near-real-time data of slope moisture conditions referred to the first meter of depth [19]. The installation of a monitoring network in this area made it possible to obtain a volumetric soil water content dataset, characterized by sufficient continuity over three years of observation (2020–2021–2022), on the basis of which it was possible to perform analyses on the correlation between soil moisture and multispectral satellite images.

2.1 Soil Moisture Monitoring Network: Characteristics and Reliability Analysis

The soil moisture monitoring network installed at the Ceriana-Mainardo site (Fig. 1) is composed of five measurement nodes (C1, C2, C3, C4 and C5), each equipped with four WaterScout SM100 sensors placed at depths of approximately −10 cm, −30 cm, 50 cm and −80 cm. The nodes are connected to a Retriever and a Modem for remote transmission of soil moisture monitoring [20] (Fig. 2).

In order to improve ground-based measurement reliability- soil moisture sensors were calibrated on the basis of the soil-specific characteristics of the area. The adopted calibration procedure is simplified and operative, as it does not properly take into account the soil porosity (for the results refer to [20, 21]). However, the monitoring network was verified to be capable of detecting the infiltration of water into the ground following a rainfall. This analysis was realized in Mendatica (Liguria, Italy), another site selected in the Ad-Vitam project, by analysing the correlation between precipitation variations (mm/h) and the volumetric water content θ (m^3/m^3%) recorded by the four sensors along

Fig. 1. Ceriana-Mainardo location.

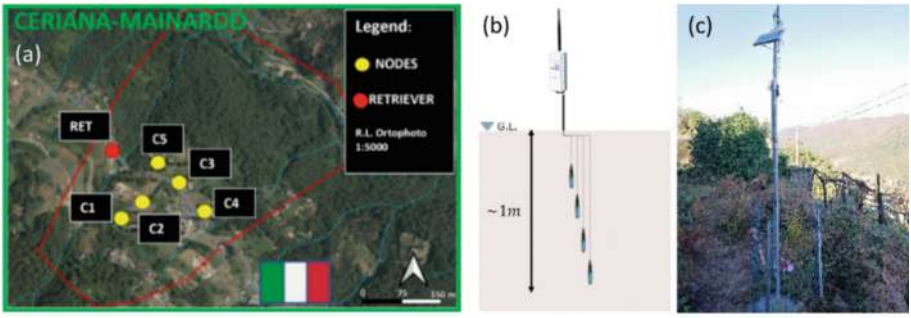

Fig. 2. (a) Soil moisture monitoring network installed in Ceriana-Mainardo. (b) Soil Moisture vertical installation mode. (c) A measurement node (C2) in *complex agriculture* Land Cover.

the vertical, forming a measurement node (called M1). Figure 3a shows an example of temporal evolution of rainfall and soil moisture measurements at the four analysed depth in January 2021. The cross-covariance (Matlab command *xcov(x,y)* [22]) between rainfall (x) and θ (y) shifted (lagged) in time, was calculated. As expected, a higher similarity between rainfall and soil moisture is evident in the shallower sensors, with maximum Pearson's coefficient (ρ) positioned at short lags (3 h). Deepest sensors show a decrease of the Pearson's coefficient (ρ), with a progressive delay of the peaks (10 cm depth: 3 h, 30 cm depth: 5 h, 50 cm depth: 6 h, 80 cm depth: 8 h), as shown in Fig. 3b for the rainfall event occurred in January 2021.

The correct functionality of the soil moisture monitoring network can be considered verified. Such an analysis makes it possible to conclude that the soil moisture dataset obtained by the described monitoring network can represent the ground-truth for further analyses. The four soil moisture datasets (concerning the four considered depths) relative to the Ceriana-Mainardo network were organized in terms of a daily median.

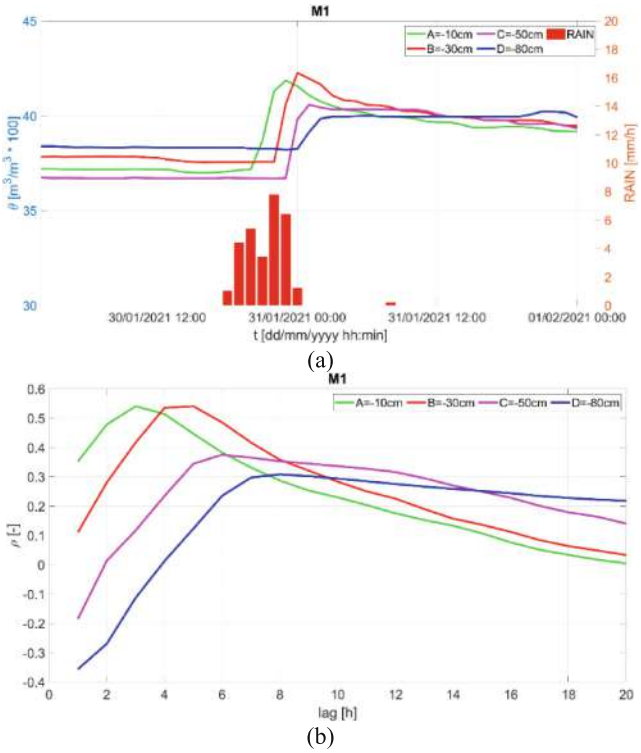

Fig. 3. (a) Rainfall and soil moisture referred to M1 node (Jan. 30–31, 2021). (b) Correlation between rainfall and soil moisture referred to M1 node (Jan. 30–31, 2021) (y-axis: Pearson's correlation coefficient ρ).

The considered time window includes the years 2020, 2021 and 2022, as it was during this period that the monitoring network operated most with the lowest number of interruptions.

3 Multispectral Images Analysis

3.1 Dataset Preprocessing

Sentinel-2 (S-2) A/B multispectral images were used in the present analysis. Automatic download of the Bottom of Atmosphere (BOA), clear sky satellite images was performed through the free script (GNU General Public License) SAme-Day SAtellite DAta Mosaics (SADASADAM) [23]. It uses the python package EODAG, distributed by the Earth Observation Data Access Gateway project [24], to search and download data, and the software FORCE (Framework for Operational Radiometric Correction for Environmental monitoring) for atmospheric correction, cloud detection, resampling and mosaic creation. Clouds are detected and eliminated, leaving only clear, usable image data. The main inputs include the coordinates of user-defined bounding box, the temporal extent and the desired percentage of cloud cover. The elaborated images, relative to

the S-2 bands at 10 m and 20 m native spatial resolution, as shown in Table 1 [25, 26], were resampled at 10 m resolution by SADASADAM [27].

Table 1. S-2 Multispectral bands processed by SADASADAM

Number	Sentinel-2 band number	Band	Center wavelength (nm)	Original spatial resolution [m]
1	2	Blue	490	10
2	3	Green	560	10
3	4	Red	665	10
4	5	Red Edge 1	705	20
5	6	Red Edge 2	740	20
6	7	Red Edge 3	783	20
7	8	Broad Near-Infrared (BNIR)	842	10
8	8a	Near-Infrared (NIR)	865	20
9	11	Short Wave Infrared 1 (SIR1)	1610	20
10	12	Short Wave Infrared 2 (SIR2)	2190	20

3.2 Processing Workflow

The adopted workflow is here presented:

1. Automatic extraction of the pixel values from the multispectral images at the selected five points relating to the measurement nodes of the soil moisture monitoring network (see yellow dots in Fig. 2a), organizing data in a unique dataset considering the vegetation as homogeneous in the study area.
2. Correlation of the reflectance (derived from the ratio of pixel values to a scaling factor of 10.000) with the soil moisture measurements relative to the day of satellite image acquisition. In particular, the multispectral images are referenced to a given time and day, while the ground-based soil moisture data are processed (as described in Sect. 2.1) to obtain daily median values. Four Reflectance – Soil Moisture datasets were thus obtained, one for each of the considered depths (−10 cm, −30 cm, −50 cm and −80 cm).
3. Outlier removal steps:
   a) for each individual multispectral band, an initial scatter plot was created with reflectance values on the x-axis and soil moisture on the y-axis; hence, an initial linear regression was created.

b) The linear regression was shifted up and down by two times the standard deviation of the reflectance, so to define a tolerance range outside of which the data are rejected. The cleaned dataset is therefore obtained (green points in Fig. 4).
c) A further cleaning was applied, defining a tolerance range of amplitude equal to the standard deviation of the previously cleaned dataset, multiplied by a factor of 1.

4. Calibration and validation of the correlations: the Reflectance – Soil Moisture datasets were randomly divided into two datasets. 70% of data was used for the definition of the Reflectance – Soil Moisture relationship calibration, considered as linear (because polynomial regression did not significantly improve the correlation in terms of increasing coefficient of determination R^2), while 30% was used for its validation and for calculation of the statistical parameters RES STD (Residual Standard Deviation) and MAE (Mean Absolute Error). An example of this phase is shown in Fig. 5 in the following section.

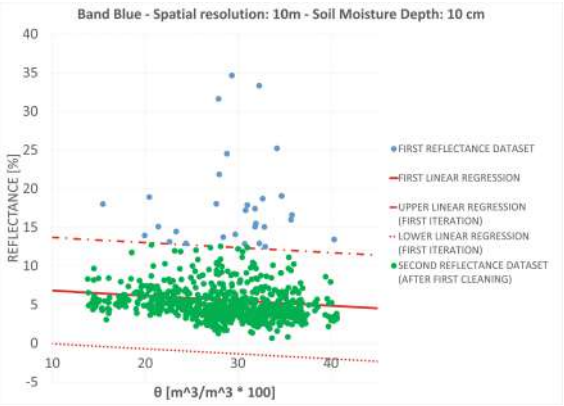

Fig. 4. Application to the blue band of outlier removal phase: First Reflectance – Soil Moisture dataset in blue points, linear regression in continuous red line, upper and lower linear regressions in dashed red lines, second reflectance dataset inside the range in green points (color figure online).

The described workflow was defined with the aim of investigating the correlations between different bands of multispectral images and soil moisture. The multiplicative factors of 2 (first iteration) and 1 (second iteration) used in outlier removal were chosen on the basis of Chebyshev Theorem [28].

4 Results

4.1 Reflectance – Soil Moisture Correlation

The processing workflow was applied to each of the available multispectral bands and to all reference depths. During the analysis, it has been noted that too low soil moisture values (<20% θ) are not always well represented by the Reflectance – Soil Moisture

correlations. According to this observation, the results reported in Tables 2, 3, 4, and 5 are related to soil moisture values above 20% θ. The best results in terms of correlation between reflectance and soil moisture are obtained for the Red Edge 2, Red Edge 3, Broad Near Infrared and Near Infrared bands at the reference depth of 10 cm, since R^2 values are higher under these conditions. Moving deeper into the soil, the correlations result weaker, as might be expected (see Tables 2, 3, 4, and 5).

Table 2. Statistical parameters obtained from the calibration (on 70% of the cleaned dataset) and validation (on 30% of the cleaned dataset) analyses of the Reflectance – Soil Moisture correlation for each band at a depth of 10 cm.

DEPTH: 10 cm			
BAND	R^2 (70% dataset)	RES STD (30% dataset) [%]	MAE (30% dataset) [%]
BLUE	0.20	4.88	4.09
GREEN	0.27	4.48	3.85
RED	0.17	4.83	4.12
RED EDGE1	0.23	4.88	4.19
RED EDGE2	**0.47**	**3.85**	**3.12**
RED EDGE3	**0.50**	**3.65**	**2.96**
BNIR	**0.48**	**3.30**	**2.85**
NIR	**0.46**	**3.55**	**3.06**
SIR1	0.20	4.59	3.87
SIR2	0.10	4.92	4.19

Table 3. Statistical parameters obtained from the calibration (on 70% of the cleaned dataset) and validation (on 30% of the cleaned dataset) analyses of the Reflectance – Soil Moisture correlation for each band at a depth of 30 cm.

DEPTH: 30 cm			
BAND	R^2 (70% dataset)	RES STD (30% dataset) [%]	MAE (30% dataset) [%]
BLUE	0.17	4.54	3.60
GREEN	0.16	4.45	3.32
RED	0.16	4.11	3.23
RED EDGE1	0.13	4.60	3.67
RED EDGE2	**0.36**	**4.36**	**3.61**
RED EDGE3	**0.37**	**3.86**	**3.09**
BNIR	**0.36**	**4.47**	**3.61**
NIR	**0.37**	**4.23**	**3.40**
SIR1	0.24	4.16	3.19

(*continued*)

Table 3. (*continued*)

DEPTH: 30 cm			
BAND	R^2 (70% dataset)	RES STD (30% dataset) [%]	MAE (30% dataset) [%]
SIR2	0.13	4.39	3.26

Table 4. Statistical parameters obtained from the calibration (on 70% of the cleaned dataset) and validation (on 30% of the cleaned dataset) analyses of the Reflectance – Soil Moisture correlation for each band at a depth of 50 cm.

DEPTH: 50 cm			
BAND	R^2 (70% dataset)	RES STD (30% dataset) [%]	MAE (30% dataset) [%]
BLUE	0.14	4.65	3.75
GREEN	0.01	5.16	4.23
RED	0.03	4.34	3.55
RED EDGE1	0.01	5.00	6.06
RED EDGE2	**0.13**	**5.07**	**4.46**
RED EDGE3	**0.25**	**5.15**	**4.44**
BNIR	**0.25**	**4.65**	**3.98**
NIR	**0.22**	**4.64**	**4.09**
SIR1	0.01	4.65	3.93
SIR2	0.00	5.46	4.60

Table 5. Statistical parameters obtained from the calibration (on 70% of the cleaned dataset) and validation (on 30% of the cleaned dataset) analyses of the Reflectance – Soil Moisture correlation for each band at a depth of 80 cm.

DEPTH: 80 cm			
BAND	R^2 (70% dataset)	RES STD (30% dataset) [%]	MAE (30% dataset) [%]
BLUE	0.15	4.33	3.53
GREEN	0.12	4.85	3.86
RED	0.15	4.33	3.55
RED EDGE1	0.10	4.37	3.63
RED EDGE2	**0.19**	**4.65**	**3.73**
RED EDGE3	**0.20**	**4.39**	**3.55**
BNIR	**0.23**	**4.16**	**3.36**
NIR	**0.23**	**4.69**	**3.72**

(*continued*)

Table 5. (*continued*)

DEPTH: 80 cm			
BAND	R^2 (70% dataset)	RES STD (30% dataset) [%]	MAE (30% dataset) [%]
SIR1	0.20	4.49	3.64
SIR2	0.12	4.54	3.75

Figure 5 shows the calibration and validation phase for the Red Edge 3 band referred to 10 cm depth. Table 6 reports the linear parameters for the calibration in Fig. 5a, while Table 7 shows the statistical parameters of the validation in Fig. 5b. Moreover, the t-test [29] was applied so to quantify how much the Observed-Estimated Soil Moisture linear regression (green line in Fig. 5b) is distant from the bisector (blue line in Fig. 5b). Table 8 shows the t-test results; note that the t-test for slope ($|t_m|$) and the t-test for intercept ($|t_q|$) are about 6 times the t-value. Even though Red Edge3 band, that is highly correlated with soil moisture (10 cm depth) ($R^2 = 0.5$), the difference between the regression line Observed-Estimated Soil Moisture and the bisector is significant.

The Reflectance – Soil Moisture correlation for Red Edge 3 band (blue line in Fig. 6) is plotted together with the regression lines at the other analyzed depths in Fig. 6. They do not change significantly with increasing depth (Table 9), except for that concerning the 80 cm depth (green line in Fig. 6).

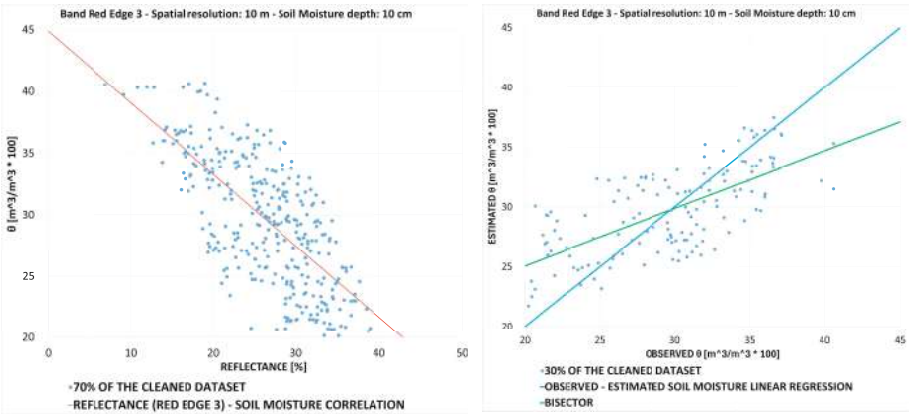

(a) (b)

Fig. 5. (a) Reflectance – Soil Moisture (Depth: 10 cm) correlation for Red Edge 3 band: the regression line is in red. (b) Validation of Reflectance – Soil Moisture (Depth: 10 cm) correlation for Red Edge 3 band: the regression line is in green, the bisector of the plan is in blue (color figure online).

Table 6. Reflectance – Soil Moisture (−10 cm) correlation for Red Edge 3 band (Fig. 5a)

Red Edge 3 band (−10 cm)				
Equation: $\theta[\%] = a \cdot REFLECTANCE[\%] + b$				
Dataset	Number of data	a	b	R^2
70% of the cleaned dataset (SM > 20% θ)	337	−0.60	44.87	0.50

Table 7. Validation of Reflectance – Soil Moisture (−10 cm) calibration for Red Edge 3 band (Fig. 5b).

Red Edge 3 band (−10 cm)				
Dataset	Number of data	RES STD	MAE	R^2
30% of the cleaned dataset (SM > 20% θ)	140	3.65	2.96	0.46

Table 8. Regression t-Test (95% confidence level) on Observed-Estimated Soil Moisture linear regression with respect to the Bisector (green and blue lines in Fig. 5b).

Red Edge 3 band (−10 cm)		
$\|t_m\|$	$\|t_q\|$	t
11.6	11.5	1.98

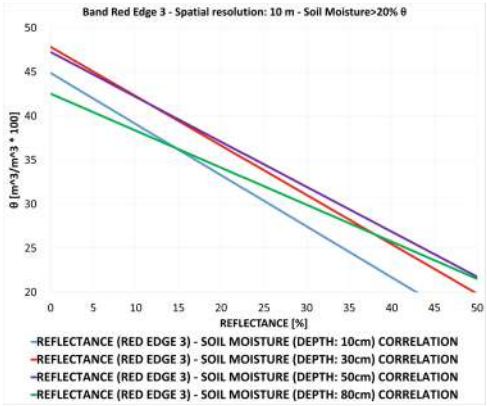

Fig. 6. Reflectance – Soil Moisture correlation for Red Edge 3 band at four analyzed depths.

Table 9. Regression t-Test (95% confidence level) on Pixel Values – Soil Moisture correlations (Red Edge 3 band) referred to 30 cm, 50 cm, 80 cm depth with respect to Reflectance – Soil Moisture correlation (Red Edge 3 band) referred to 10 cm depth

Depth	30 cm	50 cm	80 cm
$\|t_m\|$	0.52	1.29	3.67
$\|t_q\|$	3.01	1.74	1.95
t	1.97		

Spectral signature analysis at different soil moisture levels was performed, relative to 10 m depth soil moisture data. Soil moisture was expressed in terms of relative degree of saturation $S(\%) = {\theta_i - \theta_{min}}/{\theta_{MAX} - \theta_{min}}$, , in order to divide soil moisture value in classes (Class 0: $0\% < S < 20\%$, Class 1: $20\% < S < 40\%$, Class 2: $40\% < S < 60\%$, Class 3: $60\% < S < 80\%$, Class 4: $80\% < S < 100\%$). The general trend confirmed a decrease in reflectance as soil moisture increases, as shown in Fig. 7. The analysis also highlighted the difficulty of representing low levels of soil water content; in fact, class 0 is inconsistent with the trend in particular in the center part of the spectral signature, referred to the four mentioned bands best correlated with soil moisture.

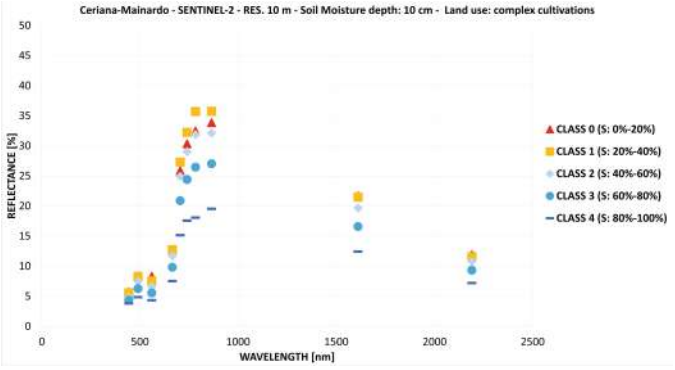

Fig. 7. Spectral signature variation related to soil moisture (depth: 10 cm)

4.2 Soil Moisture Information from Multispectral Images

The analysis of the dependencies between reflectance and soil moisture for the different multispectral bands at the different depths led to the selection of the wavelengths (Red Edge 2, Red Edge 3, Broad Near Infrared, Near Infrared) that correlate best with the variation in soil moisture, and of the reference depth best correlated with the bands (depth: 10 cm). Consequently, the proposed model can be considered valid only for Surface Soil Moisture estimate.

An even stronger Reflectance – Soil Moisture correlation is obtained considering the reflectance resulting from the mean of the four bands mentioned above, excluding

soil moisture values below 20% θ. This result is due to the removal of high frequencies determined by the mean value of the four mentioned bands. Calibration and validation of this model are shown in Fig. 8.

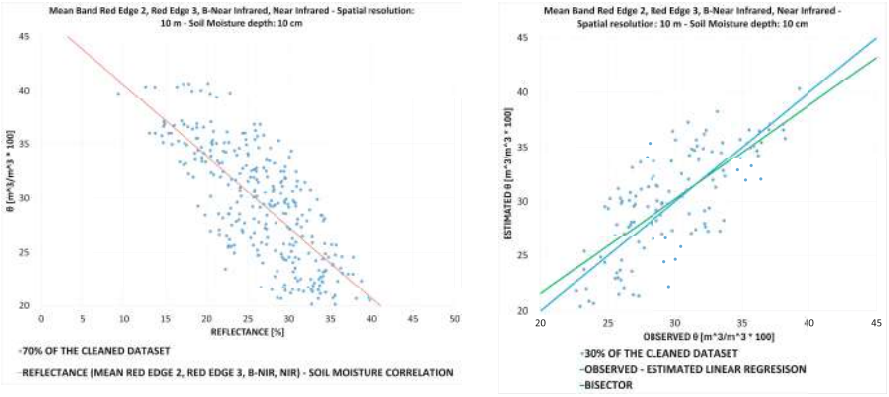

(a) (b)

Fig. 8. (a) Reflectance – Soil Moisture correlation for Mean Band (Red Edge 2, Red Edge 3, Broad Near Infrared, Near Infrared): the regression line is in red. (b) Validation of Reflectance – Soil Moisture dependency for Mean Band (Red Edge 2, Red Edge 3, Broad Near Infrared, Near Infrared): the regression line is in green, the bisector is in blue (color figure online).

The coefficients of the Reflectance – Soil Moisture correlation for Mean Band (Red Edge 2, Red Edge 3, Broad Near Infrared, Near Infrared) are reported in Table 10. RES STD and MAE values, reported in Table 11, are similar to the accuracy of the WaterScout SM100 ground soil moisture sensors (3% θ). t-test results (Table 12) show how well the Observed-Estimated Soil Moisture linear regression approximates the bisector. The present correlation allows the extraction of the SSM information at 10 cm depth relative to complex cultivations land cover, as shown in Fig. 9.

Table 10. Reflectance – Soil Moisture (−10 cm) correlation for Mean Band (Red Edge 2, Red Edge 3, Broad Near Infrared, Near Infrared).

Mean Band (Red Edge 2, Red Edge 3, B-Near Infrared, Near Infrared)				
Equation: $\theta[\%] = a \cdot REFLECTANCE[\%] + b$				
Dataset	Number of data	a	b	R^2
70% of the cleaned dataset	302	−0.7	47.10	0.56

Table 11. Statistical parameters obtained from the validation of Reflectance – Soil Moisture (−10 cm) correlation for Mean Band (Red Edge 2, Red Edge 3, Broad Near Infrared, Near Infrared).

Mean Band (Red Edge 2, Red Edge 3, B-Near Infrared, Near Infrared)				
Dataset	Number of data	RES STD [%]	MAE [%]	R^2
30% of the cleaned dataset	130	3.3	2.1	0.52

Table 12. Regression t-Test (95% confidence level) on Observed-Estimated Soil Moisture linear regression (green line in Fig. 8b) with respect to the Bisector (blue line in Fig. 8b).

Mean Band (Red Edge 2, Red Edge 3, B-Near Infrared, Near Infrared)		
$\lvert t_m \rvert$	$\lvert t_q \rvert$	t
2.4	2.5	1.98

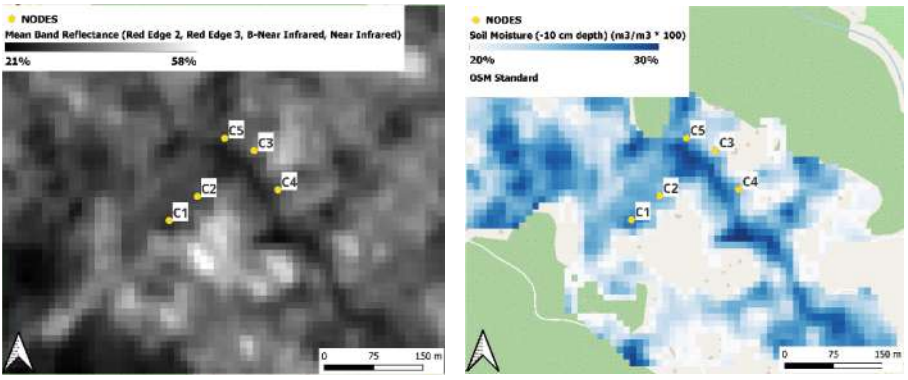

(a) (b)

Fig. 9. (a) Map representing the mean pixel values resulting from Red Edge 2, Red Edge 3, Broad Near Infrared and Near Infrared. (b) Soil moisture map (−10 cm depth, referred to complex cultivation land cover mask) obtained through the correlation in Table 10 and applying the presented workflow.

5 Conclusions

This research investigates the dependency between reflectance of multispectral Sentinel-2 images and volumetric soil water content (θ [m^3/m^3%]) variations over the Ceriana-Mainardo study area at four different depths in the first meter of soil from ground level. The analysis was developed based on the combination of two datasets, one consisting

of field measurements (considered as ground truth) of soil moisture performed using a monitoring network with capacitive sensors, the other represented by Sentinel-2 A/B multispectral images, automatically downloaded, cleared of clouds and resampled to a spatial resolution of 10 m using the SAme-Day SAtellite DAta Mosaics (SADASADAM) software. Although the study area is not characterized by bare soil, but by sparsely vegetated surfaces and complex cultivations (consisting mainly of low vegetation, i.e. herbaceous and shrub species), the results of the analysis appear encouraging.

Firstly, the spectral signature obtained at different levels of soil moisture is consistent with the literature [30, 31], which indicates the Near Infrared bands as having the highest reflectance for a vegetated surface (Fig. 7). Moreover, excluding the lowest moisture values (<20% θ), reflectance decreases as soil moisture increases, again confirming literature [32, 33].

Despite the presence of (low) vegetation on the study area, a dependency between reflectance (acquired by multispectral images) and soil moisture is manifest. It can be argued that vegetation, in this case, acts as an indirect indicator of soil moisture. The inverse proportionality between reflectance and soil moisture is confirmed by the results obtained in the correlation analysis (Figs. 5a, 6, and 8a).

The combination of the Red Edge 2, Red Edge 3, Broad Near Infrared and Near Infrared bands in their mean value led to the definition of a sufficiently strong Reflectance – Soil Moisture correlation ($R^2 = 0.56$, RES STD = 3.3% θ, MAE = 2.1% θ). Interestingly, the RES STD and MAE values are similar to the accuracy of the Water-Scout SM100 ground soil moisture sensors (3% θ) [34]. Moreover, results reported in Table 12 suggest that soil moisture values estimated with the model in Table 10 are very close to observed soil moisture, since $|t_m|$ and $|t_q|$ are a little more than one time the t-value (1.2–1.3).

This workflow has been implemented on an area mostly characterized by complex cultivations, but it can be replicated on other land uses, depending on the presence of field soil moisture data, properly installed and calibrated, in the study area for the initial model calibration. Such a procedure provides a method for the automatic SSM estimate on a large scale and with high spatial resolution, providing useful information for engineering but also, for example, agricultural applications.

Acknowledgments. Our due thanks go to Luca Delucchi and the Edmund Mach Foundation (San Michele all'Adige, Trento, Italy) for their essential help during the definition and optimisation phases of the automatic multispectral image download and processing procedure covered by this research. The authors acknowledge the support given by AD-VITAM Partners. A particular acknowledgement goes to the Unione dei Comuni della Valle Argentina e Armea and to the lab technicians of the Department of Civil, Chemical and Environmental Engineering of the University of Genoa.

References

1. Liu, Y.,et al.: Spatiotemporally non-stationary evolution of groundwater levels in Poyang Lake Basin driven by meteorological and hydrological factors. Sci. Total Environ. **950**, 175244 (2024)

2. Liu, B., Brooks, E., Mohamed, A.Z., Kelley, J.: Deep infiltration model to quantify water use efficiency of center-pivot irrigated alfalfa. J. Irrig. Drain Eng. **150**, 04024021 (2024)
3. Passalacqua, R., Bovolenta, R., Federici, B.: An integrated hydrological-geotechnical model in GIS for the analysis and prediction of large-scale landslides triggered by rainfall events. In: Lollino, G., et al. (eds.) Engineering Geology for Society and Territory, vol. 2, pp. 1799–1803. Springer International Publishing, Cham (2015)
4. Lin, R., et al.: Construction and validation of surface soil moisture inversion model based on remote sensing and neural network. Atmosphere **15**, 647 (2024)
5. Tartaglia, M., Pirone, M., Urciuoli, G.: A data-driven approach to assess the role of the groundwater conditions in triggering shallow landslides initiating with frictional failure. Landslides **20**, 1497–1517 (2023)
6. Song, Z., Li, X., Lizárraga, J.J., Zhao, L., Buscarnera, G.: Shallow landslide triggering in unsaturated vegetated slopes: efficient computation of susceptibility maps. Comput. Geosci. **154**, 104826 (2021)
7. Li, M., Sun, H., Zhao, R.: A review of root zone soil moisture estimation methods based on remote sensing. Remote Sens. **15**, 5361 (2023)
8. Babaeian, E., Paheding, S., Siddique, N., Devabhaktuni, V.K., Tuller, M.: Estimation of root zone soil moisture from ground and remotely sensed soil information with multisensor data fusion and automated machine learning. Remote Sens. Environ. **260**, 112434 (2021)
9. Adla, S., Rai, N.K., Karumanchi, S.H., Tripathi, S., Disse, M., Pande, S.: Laboratory calibration and performance evaluation of low-cost capacitive and very low-cost resistive soil moisture sensors. Sensors **20**, 363 (2020)
10. Souza, G., De Faria, B.T., Gomes Alves, R., Lima, F., Aquino, P.T., Soininen, J.-P.: Calibration equation and field test of a capacitive soil moisture sensor. In: Presented at the 2020 IEEE International Workshop on Metrology for Agriculture and Forestry (MetroAgriFor), Trento, Italy, pp. 180–184. IEEE (2020)
11. Kushwaha, Y.K., Panigrahi, R.K., Pandey, A.: Performance analysis of capacitive soil moisture, temperature sensors and their applications at farmer's field. Environ. Monit. Assess. **196**, 793 (2024)
12. Beck, H.E., et al.: Evaluation of 18 satellite- and model-based soil moisture products using in situ measurements from 826 sensors. Hydrol. Earth Syst. Sci. **25**, 17–40 (2021)
13. Plank, S.: Rapid damage assessment by means of multi-temporal SAR – a comprehensive review and outlook to Sentinel-1. Remote Sens. **6**, 4870–4906 (2014)
14. Lei, J., et al.: Prediction of soil organic carbon stock combining Sentinel-1 and Sentinel-2 images in the Zoige Plateau, the northeastern Qinghai-Tibet Plateau. Ecol. Process **13**, 32 (2024)
15. Wang, L., Gao, Y.: Soil moisture retrieval from Sentinel-1 and Sentinel-2 data using ensemble learning over vegetated fields. IEEE J. Sel. Top. Appl. Earth Observ. Remote Sens. **16**, 1802–1814 (2023)
16. Rabiei, S., Jalilvand, E., Tajrishy, M.: A method to estimate surface soil moisture and map the irrigated cropland area using Sentinel-1 and Sentinel-2 data. Sustainability **13**, 11355 (2021)
17. Zhou, T., Geng, Y., Chen, J., Pan, J., Haase, D., Lausch, A.: High-resolution digital mapping of soil organic carbon and soil total nitrogen using DEM derivatives, Sentinel-1 and Sentinel-2 data based on machine learning algorithms. Sci. Total Environ. **729**, 138244 (2020)
18. Land Cover, sc. 1:10.000, Regione Liguria Open Data Geoportal (2019). https://geoportal.regione.liguria.it/catalogo/mappe.html. Accessed 29 January 2025
19. Bovolenta, R., Passalacqua, R., Federici, B., Sguerso, D.: LAMP-LAndslide Monitoring and Predicting for the analysis of landslide susceptibility triggered by rainfall events. In: Landslides and Engineered Slopes. Experience, Theory and Practice, Proceedings of the 12th International Symposium on Landslides, Napoli, Italy, 12–19 June 2016, Volume 1, pp. 517–522. CRC Press, Taylor & Francis Group, London, UK (2016)

20. Bovolenta, R., Iacopino, A., Passalacqua, R., Federici, B.: Field measurements of soil water content at shallow depths for landslide monitoring. Geosciences **10**, 409 (2020)
21. Viaggio, S., Iacopino, A., Bovolenta, R., Federici, B.: Landslide susceptibility assessment: soil moisture monitoring data processed by an automatic procedure in GIS for 3d description of the soil shear strength. Int. Arch. Photogram. Remote Sens. Spatial Inf. Sci. XLVIII-4/W1-2022, 517–523 (2022)
22. MATLAB, Version 9.14 (R2023a). MathWorks, Natick, MA, USA
23. Gitlab Terrasigna Homepage. https://gitlab.terrasigna.com/internal/sadasadam. Accessed 15 August 2024
24. Github Homepage. https://github.com/CS-SI/EODAG. Accessed 15 August 2024
25. Hegazi, E.H., Samak, A.A., Yang, L., Huang, R., Huang, J.: Prediction of soil moisture content from sentinel-2 images using convolutional neural network (CNN). Agronomy **13**, 656 (2023)
26. Manivasagam, V.S., Kaplan, G., Rozenstein, O.: Developing transformation functions for VENμS and Sentinel-2 surface reflectance over Israel. Remote Sens. **11**, 1710 (2019)
27. FORCE Documentation Hompage. https://force-eo.readthedocs.io/en/latest/components/lower-level/level2/param.html#l2-param. Accessed 16 August 2024
28. Chebyshev, P.L.: About mean quantities. Matematicheskii Sbornik **2**, 1–9 (1867)
29. Andrade, J.M., Estévez-Pérez, M.G.: Statistical comparison of the slopes of two regression lines: a tutorial. Anal. Chim. Acta **838**, 1–12 (2014)
30. Bowers, S.A., Hanks, R.J.: Reflection of radiant energy from soils. Soil Sci. **100**(2), 130–138 (1965)
31. Gao, B.-C.: NDWI – a normalized difference water index for remote sensing of vegetation liquid water from space. Remote Sens. Environ. **58**(3), 257–266 (1996)
32. Twomey, S.A., Bohren, C.F., Mergenthaler, J.L.: Reflectance and albedo differences between wet and dry surfaces. Appl. Opt. **25**, 431–437 (1986)
33. Lobell, D.B., Asner, G.P.: Moisture effects on soil reflectance. Soil Sci. Soc. Am. J. **66**, 722–727 (2022)
34. Spectrum Technologies, Inc. Homepage. https://www.specmeters.com/WaterScout-SM100-Soil-Moisture-Sensor-20-Cable. Accessed 16 August 2024